

535-13

169333

EMPIRICAL CORRECTION FOR EARTH SENSOR HORIZON RADIANCE VARIATION

Joseph A. Hashmall,^{*†} Joseph Sedlak,^{*} Daniel Andrews,^{*}
and Richard Luquette^{*}

A major limitation on the use of infrared horizon sensors for attitude determination is the variability of the height of the infrared Earth horizon. This variation includes a climatological component and a stochastic component of approximately equal importance. The climatological component shows regular variation with season and latitude. Models based on historical measurements have been used to compensate for these systematic changes. The stochastic component is analogous to tropospheric weather. It can cause extreme, localized changes that for a period of days, overwhelm the climatological variation.

An algorithm has been developed to compensate partially for the climatological variation of horizon height and at least to mitigate the stochastic variation. This method uses attitude and horizon sensor data from spacecraft to update a horizon height history as a function of latitude. For spacecraft that depend on horizon sensors for their attitudes (such as the Total Ozone Mapping Spectrometer-Earth Probe—TOMS-EP) a batch least squares attitude determination system is used. It is assumed that minimizing the average sensor residual throughout a full orbit of data results in attitudes that are nearly independent of local horizon height variations. The method depends on the additional assumption that the mean horizon height over all latitudes is approximately independent of season. Using these assumptions, the method yields the latitude dependent portion of local horizon height variations.

This paper describes the algorithm used to generate an empirical horizon height. Ideally, an international horizon height database could be established that would rapidly merge data from various spacecraft to provide timely corrections that could be used by all.

* Computer Sciences Corporation, 10110 Aerospace Rd. Lanham/Seabrook, MD 20706, USA

† Phone (301)-794-1279, e-mail joseph.hashmall@gsfc.nasa.gov

‡ NASA Goddard Space Flight Center, Greenbelt MD, 20771, USA

INTRODUCTION

Earth horizon sensors have recently regained some of their early popularity as attitude sensors. Although they have the advantage of reliability and relatively low cost, their accuracy for near-Earth orbit missions is limited by the variability in the height of the layer of the stratosphere that they detect as the surface of the Earth's infrared spheroid. Most modern horizon sensors limit their sensitivity to radiation in the 14-16 μ band to eliminate diurnal effects and because at these wavelengths the Earth spheroid is most stable and homogeneous.

Scanning horizon sensors rotate the field-of-view (FOV) of an infrared telescope around a circular path. The sensor FOV points towards space over part of the circle and points towards Earth during the rest. The angle at which a sudden change between the low radiance of space and the high radiance of the Earth occurs is interpreted as the horizon-crossing angle. Differences and mean values of Earth-in and Earth-out horizon crossing angles can be used to provide estimates of the spacecraft pitch and roll.

Static horizon sensors have detectors that point towards the Earth horizon when the spacecraft is near its nominal attitude. The level of output from these detectors represents the portion of their FOVs that contains the Earth. Differences and means of the output from detectors viewing different portions of the horizon can be used to provide estimates of the spacecraft pitch and roll.

For both types of sensor, several effects can alter the detector output and result in attitude errors. These effects include the variation of the atmosphere's radiance in the wavelength range (roughly 14-16 μ) in which the detectors are sensitive. This paper analyzes those horizon height variations caused by those changes in radiance that result from stratospheric temperature variation. Other phenomena can also cause significant horizon sensor errors. These include the effects Earth's oblateness, of high, cold clouds, and of the proximity of the Sun or Moon image to the horizon crossing point. Some of these can easily be compensated (e.g. Earth oblateness) while others must be predicted or detected and the contaminated data removed from the processing stream. None of these other effects will be extensively discussed in this paper.

Changes in stratospheric temperatures can be interpreted as changes in the height of the infrared Earth horizon and often are the single largest uncompensated contributor to horizon sensor attitude error. These temperature changes can be classified as climatic or stochastic. In this paper the term "climatic" will be used to designate those effects that depend on latitude and season and which are repeatable from year to year. Similarly, "stochastic" will be used to designate those effects that change rapidly (over a period of days), are usually localized (over a range of a few thousand km), and are correlated in time. Stochastic effects are similar to weather and cannot be accurately predicted long in advance. For attitude determination they can best be modeled as colored noise.

Attempts have been made to analyze and mitigate the effect of the climatic variations of horizon radiance on horizon sensor attitude estimates. Extensive historical measurements of stratospheric temperatures from balloon and rocket probes have been combined with atmospheric models and electronic models of sensor triggering to produce horizon radiance models.¹ These models have been incorporated in software to compensate for the climatic variation of the infrared horizon height.^{2,3,4}

Studies of the stochastic variations of horizon radiance have shown that errors due to these variations can be as large as those due to uncompensated climatic horizon radiance

variations. Sudden stratospheric warming events⁵ can overwhelm the climatic effects in large regions of the winter hemisphere making the horizon height over a large portion of the winter hemisphere higher than that over the summer hemisphere.⁶ These events can last for as little as a few days to as much as a few weeks. Observations of the Earth infrared brightness by the GOES-8 and -9 sounders have been correlated with errors in Earth sensor based attitude control. Results show that stratospheric radiance changes can arise suddenly and can result in significant attitude errors.⁷

In preparation for the launch of the Total Ozone Mapping Spectrometer-Earth Probe (TOMS-EP), an empirical radiance modeling utility⁸ (ERMU) was developed by NASA's Goddard Space Flight Center (GSFC). This utility was to be used in an attempt to minimize the effects of horizon radiance variation on TOMS-EP attitude. This paper is a description of the results of measurements made by the TOMS-EP horizon sensors and their interpretation as changes in the Earth's infrared horizon height.

TOMS-EP was launched in July 1996 into a Sun synchronous orbit at an altitude of approximately 500 km and an inclination of 97.4 deg. After 16 months of data collection, in December 1997 it was boosted to an altitude of about 740 km and the inclination adjusted to 98.4 deg to maintain Sun synchrony. The nominal TOMS-EP attitude is Earth pointing with the Z-axis (yaw) pointing towards the Earth, the Y-axis (pitch) along the negative orbit normal, and the X-axis (roll) pointing in the general direction of the spacecraft velocity vector.

The principal attitude sensors used by TOMS-EP are two Ithaco T-scanwheel horizon sensors (HS), two fine Sun sensors (FSS), and a set of accurate rate determining gyros. The two horizon sensors are mounted with their scan axes in the Y-Z plane, canted 20 deg towards nadir from the +Y and -Y-axes respectively. Their half cone angles are 46 deg. The HSs are insensitive to Yaw so the primary Yaw information is obtained from the two Sun sensors. The Sun sensors' FOVs are directed in the +X and -X directions allowing these sensors to measure the Sun direction while the satellite is near the polar regions.

METHOD

The TOMS-EP ERMU was developed to reduce the effect of horizon radiance variation on horizon sensor performance. It was to do this by using horizon sensor data to determine horizon height variations weekly and apply the corrections needed to compensate for these variations in the following week. Although the ERMU was tested in the early phases of the TOMS-EP mission, it was never used in normal operations because its use was found to be unnecessary to meet mission requirements (0.25 deg per axis, 3σ). The approximately one year span during which horizon height variations were measured serves as an excellent reference for horizon height behavior and mitigation studies.

The basis of the ERMU horizon height measurements is the determination of the spacecraft attitude using a batch least-squares algorithm. This algorithm is implemented in GSFC's multimission three-axis stabilized spacecraft (MTASS) coarse and fine-attitude determination system (CFADS). CFADS has been used with data from many missions and has been shown to be flexible, reliable, and accurate.

The CFADS algorithm minimizes the loss function for the Wahba⁹ problem given by:

$$L = \sum_t W_s [(P_{t t_0} A_{t_0}) \hat{R}_t - \hat{S}_t]^2 \quad (1)$$

with respect to a state vector including the attitude at an epoch time and gyro biases. In Eq. (1), W_s is the relative weight of the sensor with a measurement at some time t , t_0 is the reference time, A_{t_0} is the attitude at the reference time, $P_{t t_0}$ is the transition matrix transforming the attitude at epoch to the attitude at time t (obtained by integration of gyro observations with added biases from t_0 to t), and \hat{R}_t and \hat{S}_t are reference and observed sensor measurements at time t . The sum is performed over all valid sensor measurements in a batch, including both Sun sensor and horizon sensor measurements. The primary CFADS output is the attitude of the spacecraft at times throughout the batch obtained by propagating the epoch attitude solution using gyro data modified by the determined gyro biases.

As long as the gyro biases are nearly constant (as assumed in Eq. (1) and as expected from mission experience), the attitudes obtained from CFADS will be far more accurate than single frame attitudes, and in cases with correlated errors in sensor measurements or correlated errors in reference vectors, more accurate than ordinary Kalman filters. Note that errors in horizon sensor measurements due to horizon height variations are highly correlated in time. This is because horizon height changes occur over finite areas of the Earth surface (they are correlated in space) and, therefore, measurement deviations persist while the spacecraft traverses the affected region. These correlations strongly affect the accuracy of Kalman filter derived attitudes but have little effect on the batch least-squares attitudes used in this study.

The accuracy of CFADS attitudes arises from the use of all of the sensor data in the batch. Errors arising from sensor deviations at one time can be compensated by opposing errors at other times because of gyro propagation. This compensation does not require uncorrelated errors, but increases accuracy as mean errors over the batch approach zero. In this study, an integral number of orbits were used in all CFADS batches, minimizing (due to North-South mirror symmetry) the effect of climatic horizon radiance variation.

TOMS-EP Earth sensor data is preprocessed onboard the spacecraft and reported as pitch and roll estimates for each of the two horizon sensors. They are reported every 32 seconds.

Once CFADS attitudes have been computed, sensor residuals are obtained by first computing reference roll and pitch angles. These reference angles are computed by converting the negative spacecraft position vectors to body coordinates using the corresponding calculated attitudes. The converted vectors are expressed in terms of roll and pitch angles in an nadir referenced coordinate system. Differences between these reference pitch and roll angles and the observed angles, compensated for sensor misalignment, constitute the sensor residuals.

The spacecraft orbit was divided into equal bins of orbit phase and the roll and pitch errors within each bin were averaged to give mean residuals: $\Delta \bar{r}_n$ and $\Delta \bar{\rho}_n$ for bin n . These are converted into mean horizon height deviations by the following steps:⁸

1. Compute a mean angular radius of the subtended Earth, ρ , from the nominal semimajor axis, E , the equatorial Earth radius, R_e , and the nominal horizon height, h_{nom} ($h_{nom} = 37.9$ km), by:

$$\rho = \sin^{-1} \left(\frac{R_e + h_{nom}}{E} \right) \quad (2)$$

2. Compute the nominal Earth chord width, Ω , as:

$$\Omega = \cos^{-1} \left(\frac{\cos \rho - \cos \eta \cos \psi}{\sin \eta \sin \psi} \right) \quad (3)$$

where η is the complement of the cant angle and ψ is the half cone angle.

3. Geometry coefficients for roll, K_r , and pitch, K_p , are computed from:

$$K_r = \frac{\tan \rho}{2E(\sin \eta \cos \psi - \cos \eta \sin \psi \cos \Omega)} \quad (4)$$

and

$$K_p = \frac{\tan \rho}{2E(\sin \Omega \sin \psi)} \quad (5)$$

4. Finally, the horizon height deviations for the Earth-in and Earth-out transitions are found from:

$$\Delta h_n^{in} = \frac{1}{2} \left[\frac{\Delta \bar{r}_n}{K_r} + \frac{\Delta \bar{p}_n}{K_p} \right] \quad (6)$$

and

$$\Delta h_n^{out} = \frac{1}{2} \left[\frac{\Delta \bar{r}_n}{K_r} - \frac{\Delta \bar{p}_n}{K_p} \right] \quad (7)$$

where $\Delta \bar{r}_n$ is the mean roll residual and $\Delta \bar{p}_n$ the mean pitch residual in bin n .

A minimum of four orbits of data (approximately 200 Earth observations per sensor per orbit) in each of four days were used to produce weekly averages of Earth-in and Earth-out horizon height deviations for each sensor and for each orbit phase measured from the ascending node. Horizon heights that fell within orbit phase bins having a width of 2 deg were averaged. This empirical horizon height database was produced for approximately 1 year of TOMS-EP data.

The tables of horizon heights stored by TOMS-EP orbit phase angle and week of year were designed for this single mission. Corrections to the nominal height of any of the horizon crossings were to be obtained by interpolation of phase angle using the previous weeks results. Once on orbit, it was found that this correction was not needed to attain the mission's modest attitude accuracy requirements. If one of the TOMS-EP Earth sensors fails it may be necessary to use of the ERMU to improve attitude accuracy.

To make tables of horizon heights more generally useable, and to allow compatible input from spacecraft other than the one making horizon height measurements, it is convenient to express the results in terms of the latitude of the horizon crossing rather than the phase of the spacecraft orbit. This transformation is accomplished by determining the declination angle, ρ , as:

$$\rho_n = \sin^{-1} \left(\frac{R_s + h_{nom} + \Delta h_n}{E_n} \right) \quad (8)$$

Equation (8) is virtually identical to Eq. (2) except that the oblate Earth radius beneath the (-in or -out) horizon crossing, R_s , and the true Earth to spacecraft distance, E_n , are used in place of nominal values, and the horizon height is corrected by values from the ERMU table. The geometry defining ρ is shown in Fig. 1. The location of the tangent point is obtained by finding the intersection of the nadir pointing cone with a half-cone angle of ρ and the scan cone. This

intersection consists of two possible scan vectors, \hat{S} . After selecting the correct scan vector, the vector from Earth center to this point is simply the sum of the spacecraft position vector, \vec{E}_n , and the scan vector adjusted to the correct length:

$$\vec{R}_n = \vec{E}_n + \vec{S}_n \quad (9)$$

where

$$\vec{S}_n = \hat{S}_n \sqrt{\vec{E}_n^2 - (|\vec{R}_n| + h_{nom} + \Delta h_n)^2} \quad (10)$$

The latitude, λ_n , of the tangent point can then be computed as:

$$\lambda_n = \tan^{-1} \left(\frac{\vec{R}_3}{\sqrt{\vec{R}_1^2 + \vec{R}_2^2}} \right) \quad (11)$$

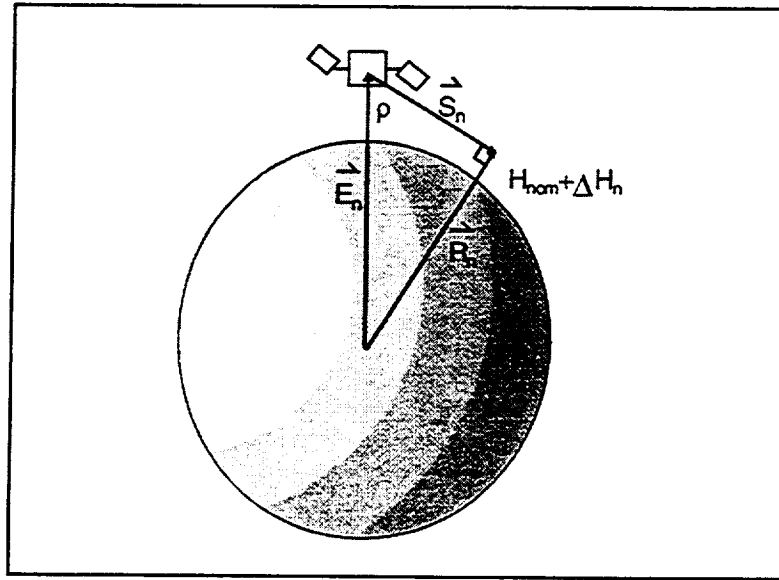


Figure 1. Geometry of Horizon Sensor Tangent Height

Strictly speaking, because of oblateness, the Earth radius is a function of the latitude of the horizon crossing, but an iterative algorithm compensating for oblateness changes latitude from the values calculated using Eq. (11) only by a negligible amount.

RESULTS AND DISCUSSION

For a period of approximately 1 year (from Summer 1996 to Summer 1997) TOMS-EP horizon sensor measurements were used to determine weekly horizon height variation tables. For each week's entries at least one orbit of data per day for at least 4 days in the week were processed. In each batch of data, observations at 32-second intervals from each of the Earth sensors were processed. A total of about 190 observations per orbit or at least 760 observations each week were used to determine Earth-in and Earth-out horizon heights for each sensor using Eqs (6) and (7). Horizon heights were collected in bins of 2 deg phase angle and averaged for each sensor and each horizon crossing (-in or -out).

The latitude corresponding to the Earth-in and Earth-out horizon crossing for the center of each phase angle bin was computed. For each week of data, horizon heights falling in the same 2-deg latitude bin were averaged even if they arose from different horizon crossings or different sensors. A contour plot showing these mean horizon heights as a function of season and latitude is presented in Fig. 2.

Individual horizon heights range from a minimum of 24.6 km to a maximum of 56.8 km. The horizon height variations with latitude and season clearly show both regular, climatic trends as well as more chaotic, stochastic effects.

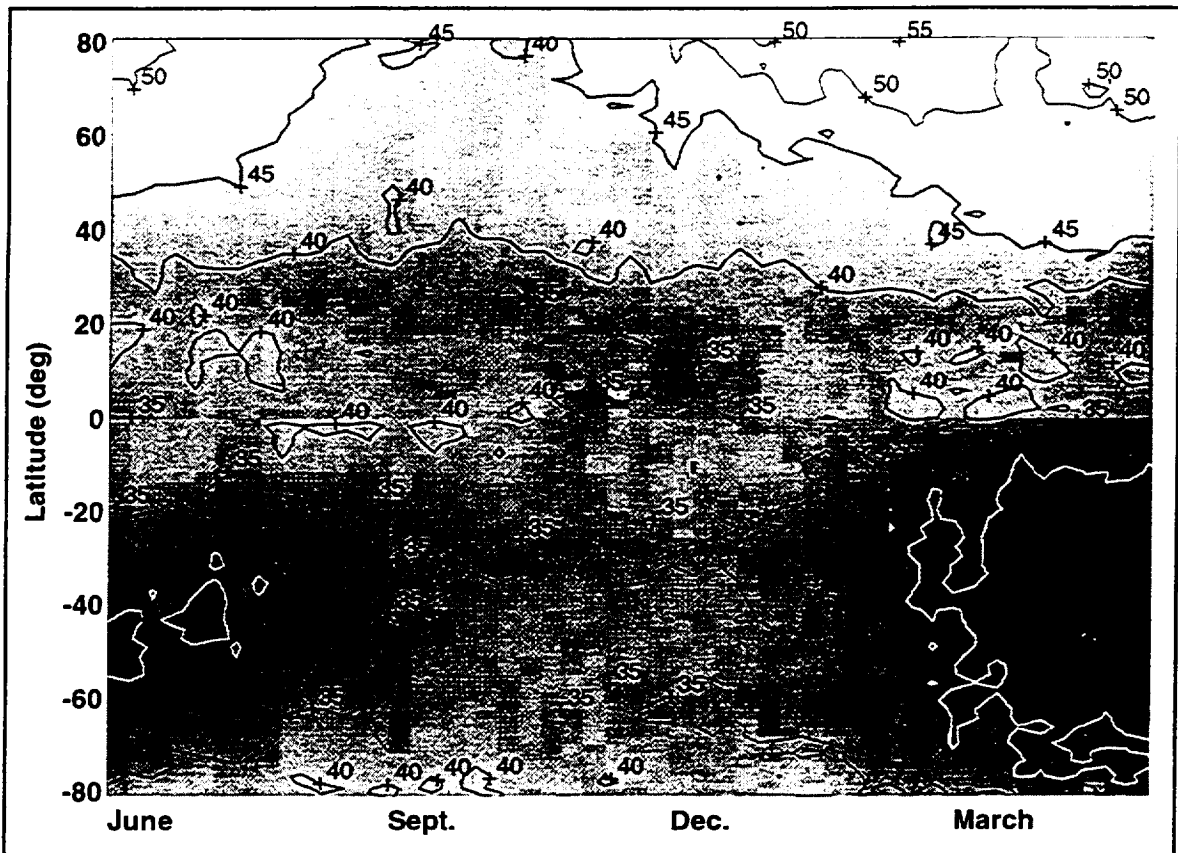


Figure 2. Measured Average Earth Sensor Horizon Heights (km) From TOMS-EP Data

The climatic effects for the study year show expected features as well as some surprising ones:

- Near the equator, the horizon height varied least throughout the year.
- In each hemisphere, there was a regular change of horizon height with season.
- Near the North Pole, the minimum horizon heights occurred in the northern autumn.
- Near the South Pole, the minimum horizon heights occurred in late in the northern spring.
- At about 50-deg south latitude, a local minimum horizon height was found in all seasons.

The stochastic effects are best demonstrated by the occurrence of numerous regions of a few weeks duration and 10 or less deg of latitude extent with average horizon heights 5 or more kilometers different from the surrounding regions.

To better describe the variation of horizon heights with time and position, weekly mean values were converted to tangent angles, ρ in Eq. (8) and Fig. 1, and the differences in these values were computed as a function of latitude for different weeks. These plots of $\Delta\rho$ against latitude for adjacent weeks, for a separation of half a year, and for a separation of approximately 1 year are presented in Fig. 3. Again, each set of weekly mean values were obtained by computed average heights (eqs. 6 and 7) using data collected during several arbitrary orbits on each of at least 4 days in each week and converting the average heights to average scanner rotation angles. The plots in Fig. 3. show differences between average scanner angles for typical weeks separated by 1 week, 26 weeks, and 1 year.

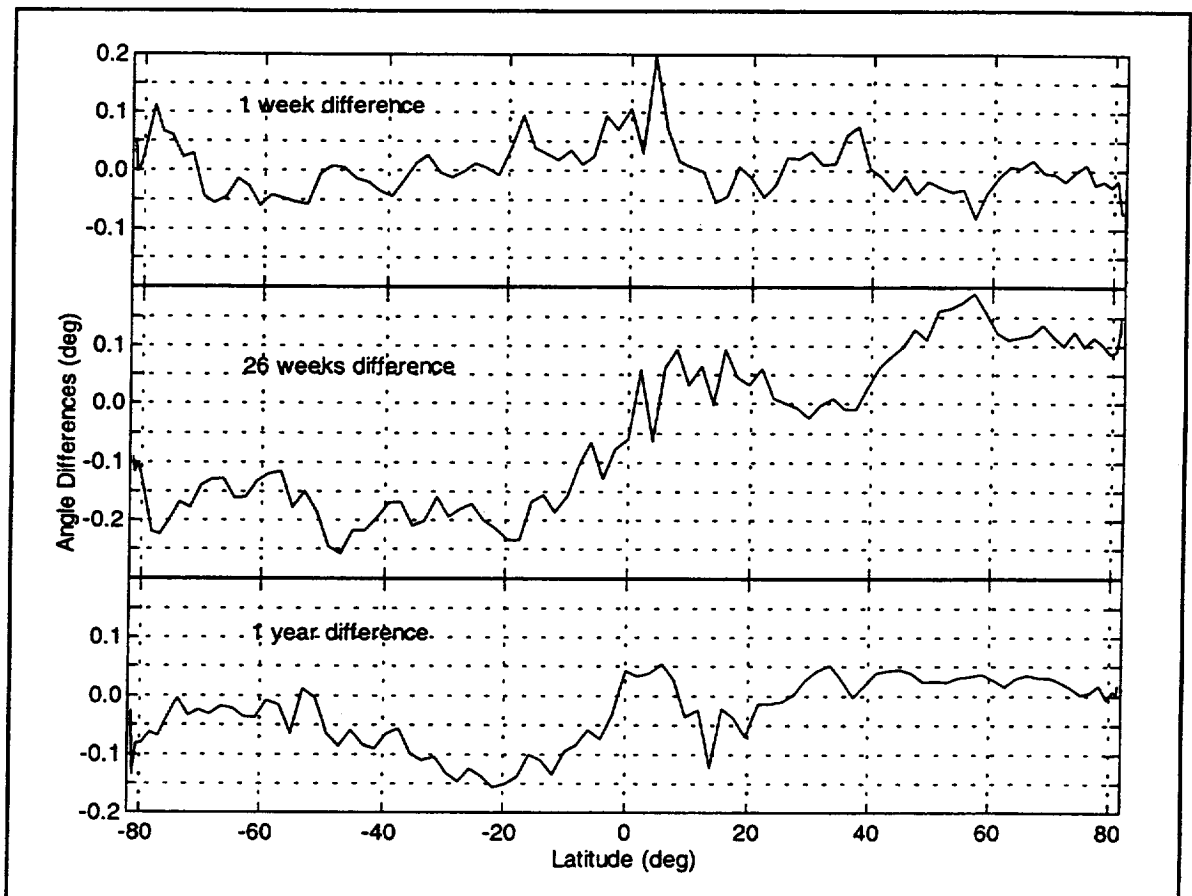


Figure 3. Tangent Angle Differences for 1 Week, 26 Weeks, and 1 Year Time Difference

In these plots, several important features of the mean tangent angles are clear:

- Values separated by either 1 week or 1 year have smaller differences than those separated by half a year.
- Values separated by half a year show the largest differences indicating clear seasonal changes.
- Values near the equator are similar, regardless of time difference.

- Values separated by 1 week are similar but large differences (≈ 0.2 deg) occur in some regions.

In order to evaluate the effect of the horizon radiance variance on attitude, TOMS-EP data for early in 1998 were examined. During this period, the spacecraft altitude had been increased to 740 km. At this altitude, horizon height variations subtend a smaller angle at the spacecraft, so the resulting measurement errors are somewhat smaller than they were earlier in the mission.

For each of 3 weeks (Feb 1-7, Feb 8-14, and March 1-7, 1998), data were processed using CFADS for 3 orbits per day on 4 or 5 days in each week. The pitch and roll residuals of each HS were accumulated and averaged in bins of 5 deg of phase angle. Data from any single day contributed an average of 8 values to each bin average. These average residuals for one day (Feb 4, 1998) are plotted against orbit phase in Fig. 4. Error bars for each bin, corresponding to $\pm 1\sigma$ deviations from the mean, are also included in this figure.

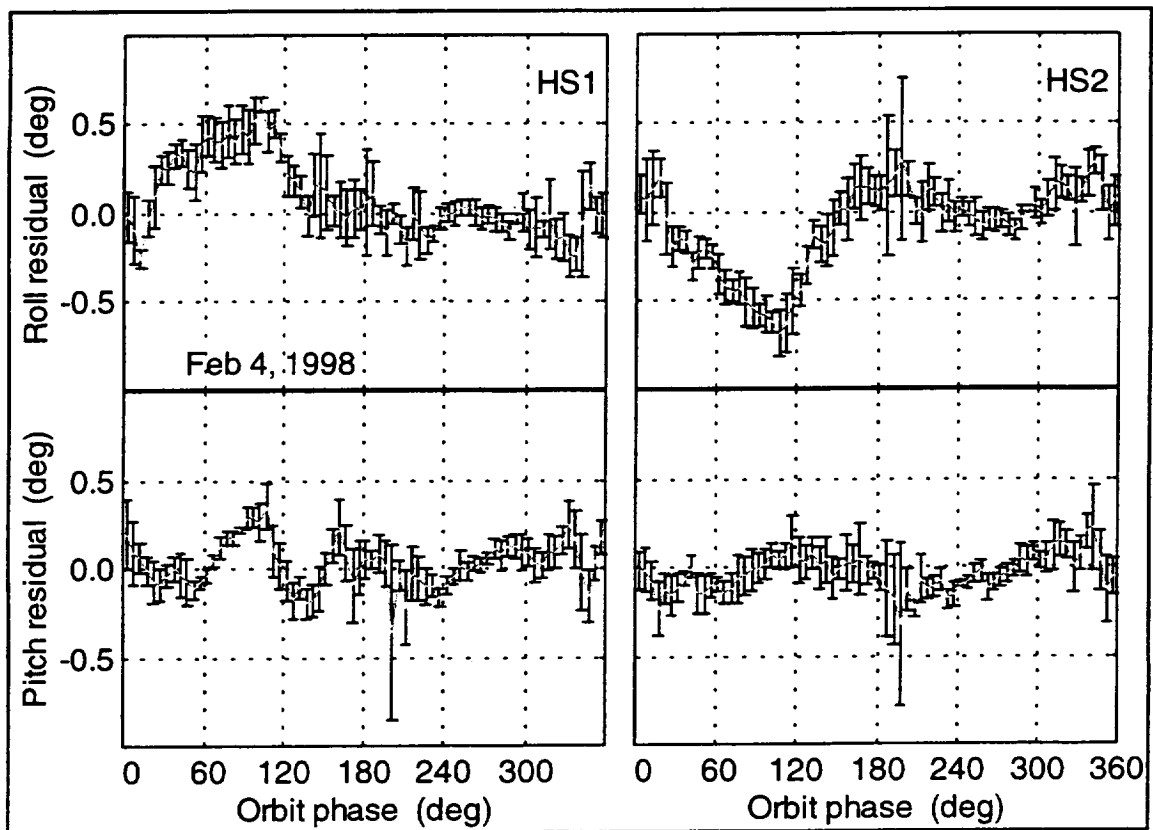


Figure 4. Mean TOMS-EP Roll and Pitch Errors for Feb 4, 1998

Several interesting features are apparent in these plots:

- Single sensor roll and pitch errors can have residuals that are as large as 0.5 deg.
- Residuals show systematic variations with orbit phase.
- The standard deviations of the residuals in any orbit phase bin may differ by large amounts from those in other bins.

- Noisy bins (those with large standard deviations) seem to be clustered near each other, as are bins with small standard deviations.
- The noisiest bins are clustered in the same general region of the orbit (phase near 200 deg) for both of the sensors.

These observations can be explained by the existence of regions of unusual horizon height. At phase angles in an orbit where one or the other of the horizon crossings for a HS passes through such a region large residuals are produced. If the region is localized in longitude, the horizon crossing on subsequent orbits will not be affected, producing large standard variations of the mean. At other phase angles, where no anomalous horizon height regions are observed, the standard deviations will be smaller.

Were this explanation true, the plots in Fig. 4 would change in an unusual manner as more data from other days is added. In cases with normal distributions of measurements, adding data should systematically reduce the standard deviations. Assuming normal distribution, adding 4 additional days of data to the one day shown in Fig. 4 should decrease the standard deviations to less than half their previous values. The actual changes are shown in Fig. 5. In the plots shown in this figure, each bin represents an average of about 40 observations.

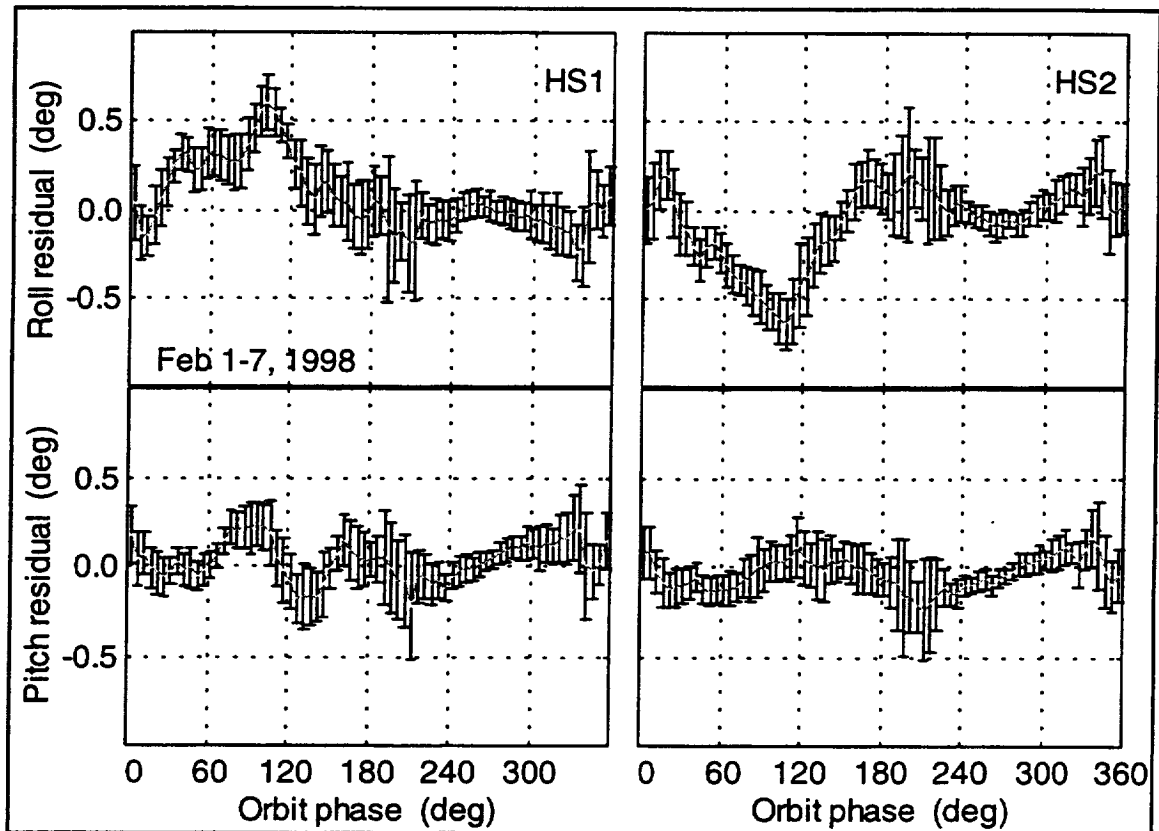


Figure 5. Mean TOMS-EP Roll and Pitch Errors for Feb. 1-7, 1998

It is clear from this figure that adding more data increases the standard deviations at most orbit phases. This result is consistent with the growth and decay of anomaly regions within the week period covered by each plot. As a new anomaly region grows it changes the residuals

during the portion of some orbits. This increases the standard deviations and shifts the mean. The same effect occurs as the region disappears.

Also for most values of phase angle, adding data from different days reduces the differences in standard deviations among adjacent bins. Even with this smoothing, for some regions (e.g. near 200-deg phase angle in the week of Feb. 1) the standard deviations are consistently large, while for others (e.g. between 240 and 300 deg phase) the standard deviations are consistently low.

Figures 6 and 7 show similar averages obtained from data in the following week (Feb. 8-14, 1998) and three weeks after that (March 1-7, 1998), respectively.

In the plots representing HS1 residuals in the week of Feb. 8-15, there are exceptionally large values of the mean residual as well as standard deviations near 200 deg phase angles. Most of these large values can be traced to short periods (1-2 minutes in duration) during which HS1 measured anomalous values. These roll and pitch values were more than 1 deg from nominal, lasted for several measurement periods, and occurred on at least 2 days. They were not observed in every orbit and, although their approximate position remained the same, moved by several deg of orbit phase from day to day.

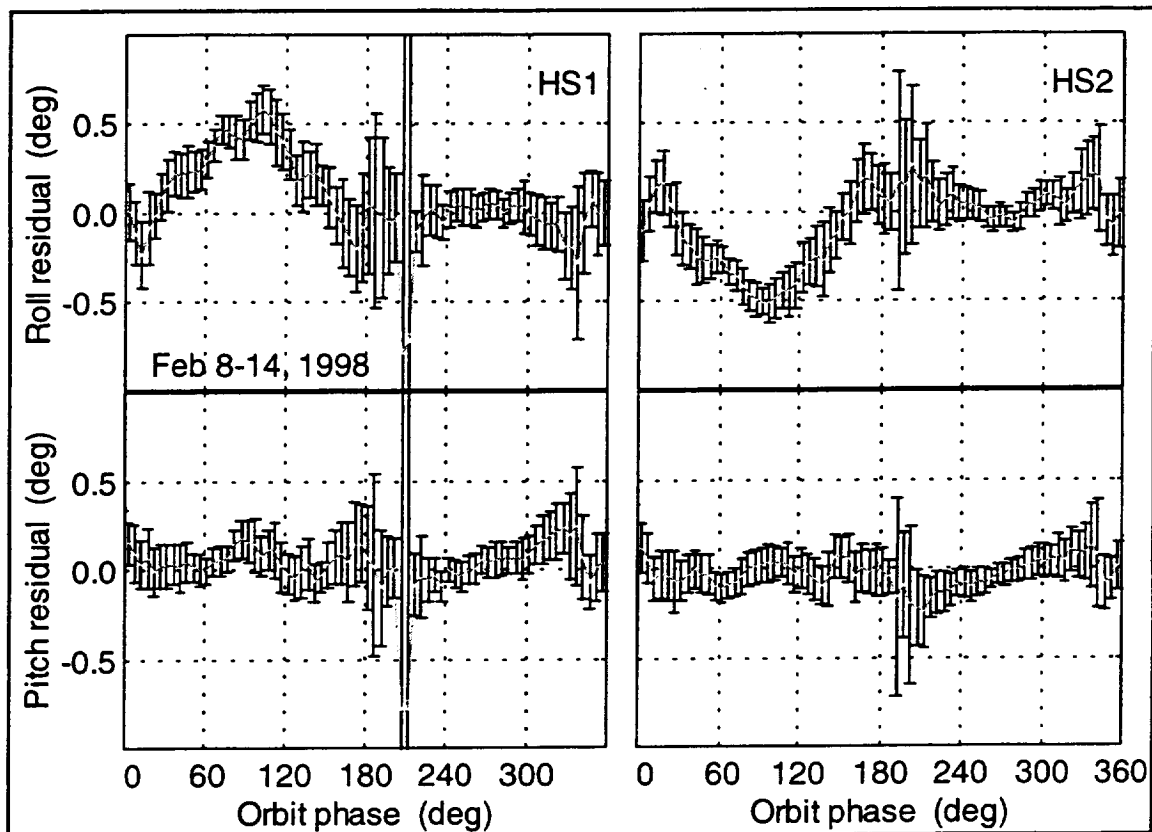


Figure 6. Mean TOMS-EP Roll and Pitch Errors for Feb. 8-14, 1998

There are many possible causes for the anomalous behavior near 200 deg phase angle. It is well known that the presence of the Sun or Moon near the position where a HS detects the horizon can cause large errors in attitude measurements.¹⁰ Although Sun and Moon interference

can cause pitch and roll errors of this size, examination of standard TOMS-EP HS interference utility results show no Sun or Moon interference for at least 24 hours before and after these anomalies. High, cold clouds can also cause HS errors,¹¹ but the size of these errors is usually limited to a 0.1-0.2 deg. Other possible causes for this anomaly, including Sun glint, shading, etc. were not investigated.

These anomalies probably are not an artifact of telemetry processing because the moderately large standard deviations in HS2 for the same period and phase angle are probably due to a response to HS1 anomalies by the OBC attitude control system. The facts that they recur at approximately the same phase angle on adjacent days, and that they contain more than a single observation each, makes it likely that these anomalies are caused by a physical phenomenon.

Except for the anomalous portions of the data in the week of Feb. 8-14, the mean values of horizon sensor residuals are quite similar from week to week. Differences of about 0.1 deg can be seen (for example near 125 to 175 deg of phase angle in the plot of pitch residuals). The size of these differences is consistent with the results shown in Fig. 3.

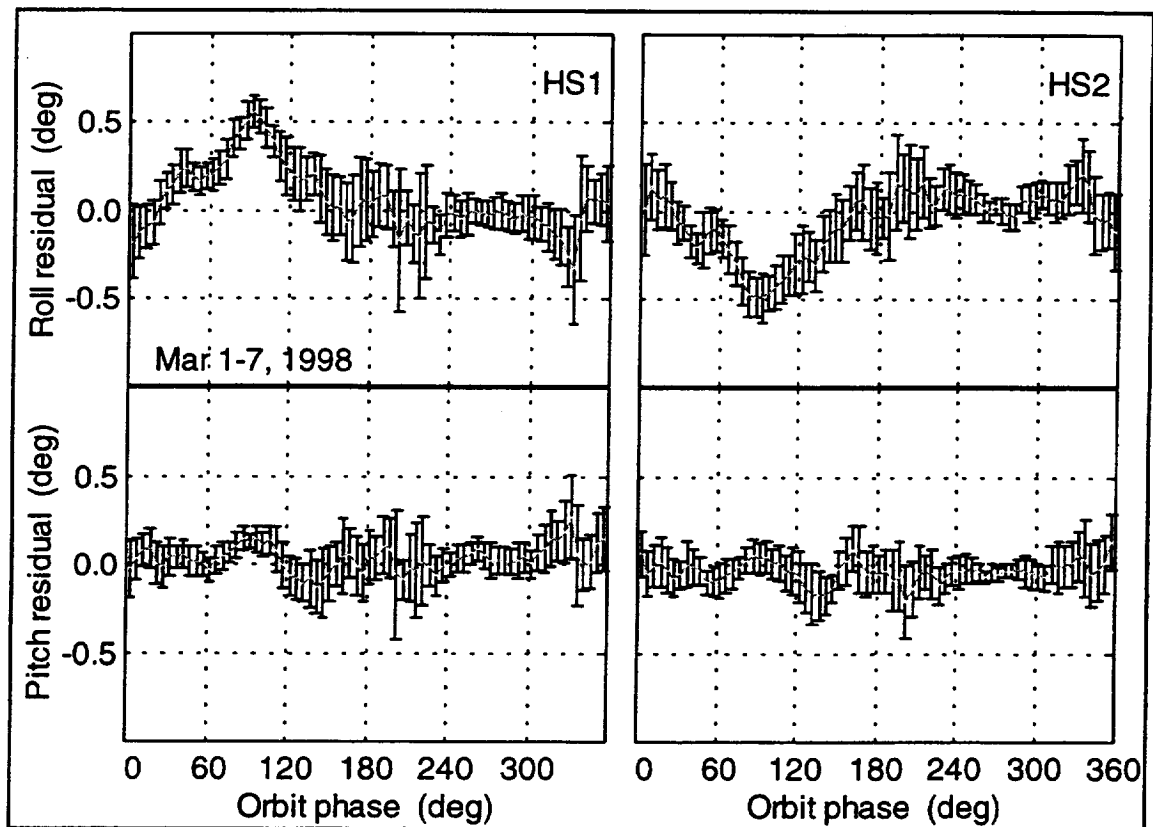


Figure 7. Mean TOMS-EP Roll and Pitch Errors for March 1-7, 1998

The standard deviations are consistently larger in some portions of the orbit and smaller in others. The mean of the standard deviations over all of the phase angle bins, both of the sensors, and both attitude directions is about 0.15 deg. This value reveals more about the fraction of the time during which a HS will have relatively large errors than it does about either the random noise the sensor will experience or the reliability of a horizon height model.

The relative size of the residuals throughout any orbit also shows a consistent pattern. Much of this pattern can be explained by the positions of the HS horizon crossing points as a function of orbit phase. The latitudes of these positions (using a nominal orbit and nominal horizon heights) are shown in Fig. 8

When the -in and -out horizon crossings for both HSs fall at nearly the same latitude (e.g. near orbit phases of 90- and 270-deg), the standard deviations are smaller than in regions where the horizon crossings fall at different latitudes. The largest standard deviations in all of the weeks occur between orbit phases of 180 and 240 deg. where one of the horizon crossings is approaching the summer pole and the other remains at much lower latitudes.

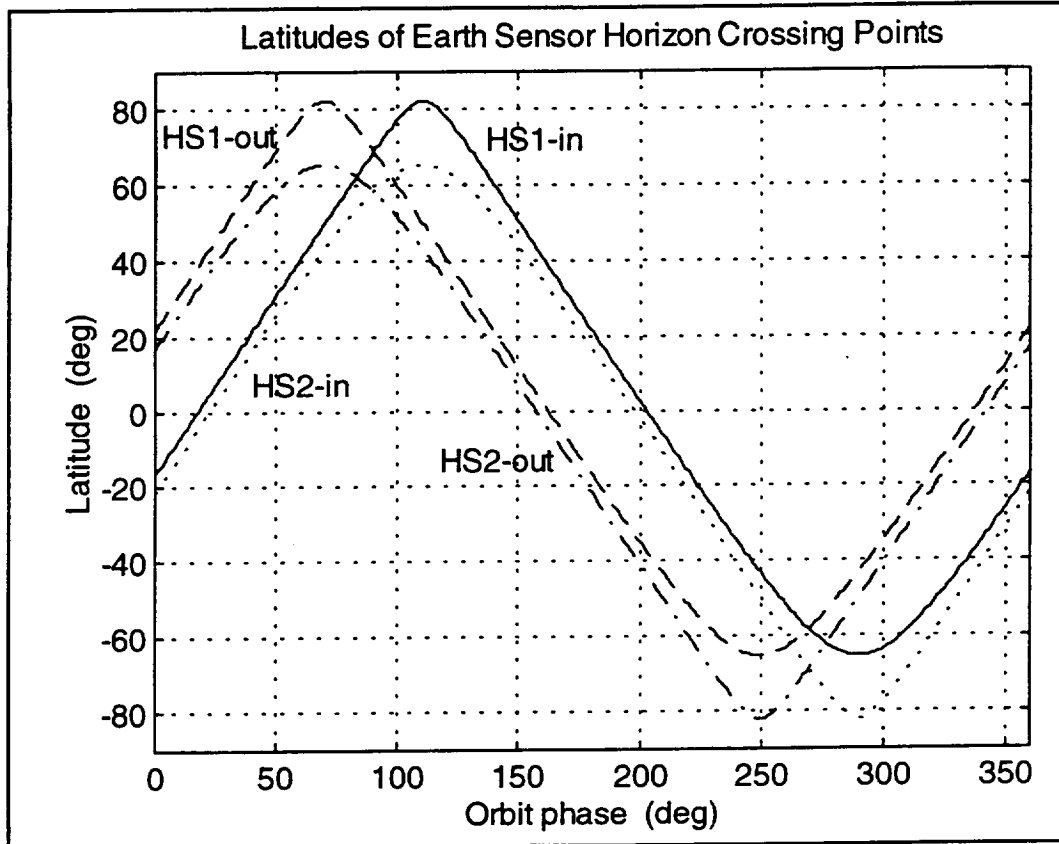


Figure 8. Horizon Crossing Latitudes vs. Phase Angles for a Nominal TOMS-EP Orbit

CONCLUSIONS

The data presented here as well as that cited from earlier studies is consistent with a horizon height model that includes climatic and stochastic effects of approximately the same importance. The climatic effects are, by definition, predictable and can therefore be reduced through the proper use of models. The stochastic effects can not be predicted and their effects can not therefore be completely removed.

Stochastic effects are localized in both time and space and introduce colored noise into the horizon radiance. Treating these effects as uncorrelated noise with normal distribution

produces sensor error models that, although convenient to use, are not optimal since they do not accurately reflect the system's statistics.

When evaluating the accuracy of a sensor in the design phase of a mission, that sensor's measurement error statistics should be used explicitly to evaluate the probability that a certain level of attitude error will occur. Because the horizon height variation contains a significant contribution from sequentially correlated errors, the assumption of white noise and use of the corresponding simple standard deviation as a measure of sensor error yields a misleading description of attitude errors.

Given the observed error distribution on TOMS-EP, it is probable that in any orbit there will be regions in which the sensor error will be much higher than the standard deviation obtained from statistics on measurements over many orbits, many days, and even many years. Using more observations to determine the standard deviation may refine this value but will not help to determine the fraction of each orbit that the sensor (and the spacecraft attitude) can be expected to have large errors.

The effect of correlated sensor errors cannot easily be removed by the typical Kalman filters used for spacecraft attitude determination. These filters give optimal results assuming uncorrelated, gaussian-distributed noise. Although the inherent sensor noise may indeed be random and white, the sensor and attitude residuals contain contributions from the colored errors in the Earth horizon height model. In a similar case, that of correlated errors in magnetic field models, a filter that explicitly accounts for correlated noise has been developed and has improved attitude determination markedly.¹²

Several approaches are currently being pursued to evaluate and mitigate horizon radiance errors on Earth sensor derived attitudes. These include:

- development and testing of a correlated noise filter
- evaluation of the attitude accuracy improvements that can be expected in Kalman filters and through use of a system similar to the ERMU
- evaluation of the attitude accuracy improvements that can be expected in batch-least squares methods using a system similar to the ERMU
- evaluation of the attitude accuracy improvements that can be expected in Kalman filters by ignoring HS measurements with high latitude horizon crossing.

Many factors not discussed here affect the height at which a horizon sensor detects the Earth. These include the trigger logic and rotation rate for scanning HSs as well as the size and shape of the instantaneous FOV and the sensor mounting geometry. Differences from nominal triggering height at a particular location on the Earth's surface should be more nearly equivalent for different missions than are the heights themselves.

If a system like the ERMU proves to be successful in reducing attitude errors to a level lower than attainable with climate models, input to horizon height correction tables from many spacecraft might be desirable. In this case, weekly horizon radiance correction tables might be generated and used by each contributing spacecraft to correct its horizon height model and improve its attitude accuracy.

ACKNOWLEDGMENTS

This work was supported by the National Aeronautics and Space Administration (NASA)/ Goddard Space Flight Center (GSFC) under contracts NAS 5-31000 and GS-35F-4381G, task order No. S-03365-Y.

REFERENCES

1. M. C. Phenneger, S. P. Singhal, T. H. Lee, and T. H. Stengle, "Infrared Horizon Sensor Modeling for Attitude Determination and Control: Analysis and Mission Experience," NASA, TM 86181, March 1985.
2. W. Nutt and M. C. Phenneger, "Horizon Radiance Modeling Utility System Description and User's Guide," *Computer Sciences Corporation*, CSC/SD-78/6032, March 1978.
3. E. J. Burgess, "Earth Radiation Budget Satellite (ERBS) Horizon Radiance Modeling Utility (HRMU) User's Guide and System Description," *Computer Sciences Corporation*, CSC/SD-84/6007, June 1984.
4. R. Shendock, "DE-B Horizon Radiance Modeling Utility (HRMU) System Description and User's Guide," *Computer Sciences Corporation*, CSC/SD-80/6096, 1980.
5. S. Fritz and S. D. Soules, "Planetary Variations of Stratospheric Temperatures," *Monthly Weather Reviews*, Vol. 110, no. 7, July 1972.
6. E. Harvie, O. Filla, and D. Baker, "In-Flight Measurement of the National Oceanic and Atmospheric Administration (NOAA)-10 Static Earth Sensor Error," *AAS/AIAA Spaceflight Mechanics Meeting*, Pasadena, CA. AAS 93-101, Feb. 1993.
7. M. C. Phenneger, W. C. Bryant, J. Baucom, and K. Woodham, "Evaluating the Goes-8 & -9 Earth IR Horizon Sensor Error Response Using the Goes-9 Sounder IR Channel 1 thru 4 Data," *Proc. SPIE*, Vol. 2812, Oct. 1996.
8. S. Shulman, *et al.*, "Total Ozone Mapping Spectrometer-Earth Probe (TOMS-EP), Flight Dynamics Support System (FDSS), Functional Specifications," (revised version) *Computer Sciences Corporation*, CSC/TR-92/6008R1UD0, Nov. 1993.
9. G. Wahba, "A Least-Squares Estimate of Spacecraft Attitude," *SIAM Rev.* Vol. 7, No. 3, July 1965.
10. M. C. Phenneger, S. P. Singhal, T. H. Lee, and T. H. Stengle, *op. cit.*, Sec. 4.
11. *ibid.*
12. J. Sedlak, "Improved Spacecraft Attitude Filter Using a Sequentially Correlated Magnetometer Noise Model," *Proceedings of the 16th Digital Avionics Subsystems Conference*, Irvine CA, October 1997.

